PROCEEDINGS OF SCIENCE

Disentangling the multi-messenger puzzle of the AGN-starburst composite galaxy NGC 1068

Björn Eichmann,[a,b,*] **Foteini Oikonomou,**[c] **Silvia Salvatore,**[a,b] **Ralf-Jürgen Dettmar**[b,d] **and Julia Becker Tjus**[a,b,e]

[a] *Ruhr-Universität Bochum, Theoretische Physik IV, Fakultät für Physik und Astronomie, Bochum, Germany*
[b] *Ruhr Astroparticle and Plasma Physics Center (RAPP Center), Bochum, Germany*
[c] *Norwegian University for Science and Technology (NTNU), Institutt for fysikk, Trondheim, Norway*
[d] *Ruhr-Universität Bochum, Astronomical Institute, Fakultät für Physik und Astronomie, Bochum, Germany*
[e] *Department of Space, Earth and Environment, Chalmers University of Technology, 412 96 Gothenburg, Sweden*

E-mail: eiche@tp4.rub.de

The recent observation of tera electronvolt neutrinos from NGC 1068 has clarified that the dominant high-energy neutrino sources might actually be gamma-ray dim at these energies. But to understand the whole multi-messenger picture, we need not only to account for the central region of this active galactic nucleus (AGN) but also for its circumnuclear starburst region. In this work, we update a recently published multi-messenger model for AGN-starburst composite galaxies by a detailed treatment of the stochastic acceleration process within the AGN corona. Moreover, we introduce some updates of the multi-messenger data and show that the entire spectrum can still be described very well if both, starburst *and* AGN corona, are taken into account. In contrast to the previous results a significantly lower CR pressure within the corona is needed and a strong decline of the neutrino flux towards lower energies at about 1 TeV is obtained.

38th International Cosmic Ray Conference (ICRC2023)
26 July - 3 August, 2023
Nagoya, Japan

ICRC2023
38th International Cosmic Ray Conference
The Astroparticle Physics Conference

[*] Speaker

https://pos.sissa.it/

PoS(ICRC2023)1453

1. Introduction

The recent observation of high-energy neutrinos from the Seyfert galaxy NGC 1068 by the IceCube experiment [1] clarified that these sources are of special interest for the high-energy astrophysics community—as potential sources of highly-energetic cosmic rays (CRs) and their associated by-products in form of electromagnetic radiation and high energy neutrinos. Since many Seyfert galaxies do not show (at least for many years) any clear sign of non-thermal activity, this finding caused some rethinking within the community. As NGC 1068 is the brightest and one of the closest Seyfert type 2 galaxies there have also been models that predicted it to be one of the brightest neutrino sources in the northern hemisphere [2]. To some surprise the actually observed neutrino flux lacks an electromagnetic counterpart at these energies. Thus, the production side seems to be opaque for γ-rays above some hundreds of GeV. Moreover, NGC 1068—as well as several other Seyfert galaxies—features a starburst region, which is characterized by a high rate of star formation and supernova explosions, and it is therefore referred to as active galactic nuclei (AGN)-starburst composite galaxy. Here, the starburst is located in a circumnuclear ring-like structure with a radius of about 1 kpc with respect to the AGN in its center. Hence, at low frequencies, i.e. up to the X-ray regime, current observatories have actually a sufficient spatial resolution to distinguish the two potential emission sites of NGC 1068. But the detailed origin of the observed high-energy γ-radiation by the *Fermi*-Large Area Telescope (LAT) as well as the high-energy neutrinos at even higher energies is unclear. Indications that a one-zone model is not enough to explain the multi-messenger emission from NGC 1068 have been present for several years, e.g. [3]. But the recent high-energy neutrino signal with the missing γ-ray counterpart clearly exposes the need for a second source environment that generates the γ-ray flux up to some tens of GeV. In contrast to the neutrino origin that is commonly considered to be associated to the AGN corona [4–7]—due to the need for an opaque environment where CR particles could be accelerated up to at least some tens of TeV—the origin of the GeV γ-rays is still under debate: Since NGC 1068 also possesses a jet-like structure on sub-kpc scales as indicated by centimeter radio observations [e.g. 8, 9] it has been suggested [10] that the observed gamma-rays originate in these jets as a result of CR electrons inverse Compton scattering off the infrared (IR) radiation from the torus. Or alternatively, winds from the coronal region that impact the torus and trigger shocks enable CR protons to be accelerated up to TeV energies, so that the observed GeV photons originate from hadronic pion production with the torus gas [11]. In this work we account for the circumnuclear starburst ring as the potential source of the GeV γ-rays. In addition, we model the AGN corona and use the multi-messenger data of NGC 1068 to disentangle the multi-messenger puzzle of that source. In contrast to the previous approach [7], hereafter referred to as E+22, we have updated the data sample and improved the treatment of the stochastic acceleration process within the AGN corona.

2. AGN-starburst model

In the following we adopt the two-zone AGN-starburst model of E+22 for NGC 1068: An inner spherically symmetric AGN corona with a radius of some tens of Schwarzschild radii $\mathcal{R}_s = 2GM/c^2$ as well as an outer starburst ring with a radius of ~ 1 kpc. Both spatial regions seem to be in steady state and they are treated as spatially homogeneous for mathematical convenience. Moreover, we account for a magnetic field (that is uniform on small scales and randomly orientated on significantly larger ones), a constant thermal gas target density $n_{\rm gas}$ with a temperature $\theta_{\rm gas}$ and an energy dependent thermal background photon target. More details on these ingredients can be found in E+22.

In the case of the starburst ring (str), the acceleration is expected to be introduced by a multitude of supernova remnants (SNRs) via diffusive shock acceleration (DSA). Here, the CRs with momentum p are kept within the accelerating shock region of magnetic field strength B by the Bohm diffusion, due to the CR self-generated Bell instability, so that the acceleration timescale yields, e.g. [12], $\tau_{\rm acc}^{\rm str} \simeq 20/3\,(p/e\,B)\,\,(c/v_{\rm sh})^2$. Here, the average shock speed $v_{\rm sh}$ can be assumed to equal the wind speed $v_{\rm w}$, e denotes the elementary charge and c refers to the speed of light. Considering the commonly used two-zone approach[1] for the starburst region, where DSA within the acceleration zone yields a primary source rate $q^{\rm str}(p) \propto p^{-s}\,\exp[-p/\hat{p}]$ of relativistic electrons and protons, respectively, with a momentum p and a spectral index with $1.5 \lesssim s \lesssim 2.5$ as expected from conventional DSA. The maximal momentum $\hat{p}$ is determined by the equality of the acceleration and loss timescales, i.e. $\tau_{\rm acc}^{\rm str}(\hat{p}) = \tau_{\rm loss}^{\rm str}(\hat{p})$. Hereby, $\tau_{\rm loss} = [\tau_{\rm cool}^{-1} + \tau_{\rm esc}^{-1}]^{-1}$, where $\tau_{\rm cool}$ and $\tau_{\rm esc}$ denote the relevant cooling and escape timescales, respectively, as given in E+22. The normalization of the proton injection rate can be obtained from

$$c\,V^{\rm str} \int {\rm d}p'\;\, p'\, q_{\rm p}^{\rm str}(p') = \nu_{\rm SN}\, f_{\rm SN}\, E_{\rm SN}\,, \tag{1}$$

based on the given supernova rate $\nu_{\rm SN}$ and the fraction $f_{\rm SN}$ of the total ejected energy $E_{\rm SN}$ of the supernova that goes into CRs within the volume $V^{\rm str}$ of the starburst ring. Thus, the acceleration zone provides a primary source rate for the interaction zone, where the CRs subsequently suffer from continuous and catastrophic energy losses yielding a steady state density distribution $n^{\rm str}(p)$ according to

$$-\frac{\partial}{\partial p}\left(\frac{p\, n^{\rm str}(p)}{\tau_{\rm cool}^{\rm str}(p)}\right) + \frac{n^{\rm str}(p)}{\tau_{\rm esc}^{\rm str}(p)} = q^{\rm str}(p)\,\left(+q_{\rm e^\pm}^{\rm 2nd}(p)\right)\,. \tag{2}$$

Here $q_{\rm e^\pm}^{\rm 2nd}(p)$ denotes the additional (leptonic) contribution by secondary electrons (e^-) and positrons (e^+) that are generated by hadronic interaction processes.

In the case of the corona region (cor), however, the acceleration is expected to result from stochastic diffuse acceleration (SDA), where the same scattering process that yields the diffusive escape is also responsible for the stochastic acceleration. Thus the corresponding the acceleration timescale is given by, e.g.[5],

$$\tau_{\rm acc}^{\rm cor} \simeq \eta\,\left(\frac{c}{v_{\rm A}}\right)^2\,\frac{R}{c}\,\left(\frac{pc}{e\,B\,R}\right)^{2-\varkappa}\,, \tag{3}$$

where we consider turbulence with a power spectrum $\propto k^{-\varkappa}$ and a turbulence strength η^{-1}. Commonly it is assumed that either $\varkappa = 5/3$ referring to Kolmogorov turbulence, or $\varkappa = 3/2$ (Kraichnan turbulence), which can be motivated from isotropic MHD turbulence in the magnetically dominated regime, if it is realized. Moreover, $v_{\rm A} = B/\sqrt{4\pi\, m_{\rm p}\, n_{\rm gas}}$ denotes the Alfvén speed, which depends on the given magnetic field strength B as well as the number density $n_{\rm gas}$ of thermal protons of

[1]Not to be confused with the two-zone AGN-starburst model that was mentioned earlier.

mass $m_{\rm p}$. Note that the Alfvén speed is also the crucial quantity to determine the development of the turbulence cascade, which happens on timescales $\tau_{\rm cas} \sim R/v_{\rm A}$. Since, efficient SDA needs turbulence on small scales (large wavenumbers k), the infall time $\tau_{\rm inf} = R/a_{\rm vis} v_{\rm K}$, which depends on the dimensionless viscosity parameter $a_{\rm vis}$ and the Keplerian velocity $v_{\rm K} = \sqrt{G\,M_{\rm BH}/R}$, needs to be large enough, i.e. $\tau_{\rm inf} > \tau_{\rm cas}$.

In case of SDA within the corona, the previously mentioned two-zone model is no longer valid, as there is no spatially confined acceleration zone. Hence, one has to include momentum diffusion in the transport equation (2), so that however, a semi-analytical solution is only possible under certain conditions. One of these conditions, as shown by Ref. [13], is an inefficient particle escape, i.e. $\tau_{\rm cool} \ll \tau_{\rm esc}$—as expected in case of the corona (see e.g. E+22). Therefore, we solve the steady state transport equation

$$\frac{\partial}{\partial p}\left[\left(\frac{2D(p)}{p} - \frac{p}{\tau^{\rm cor}_{\rm cool}(p)}\right) n^{\rm cor}(p)\right] - \frac{\partial}{\partial p}\left[D(p)\frac{\partial n^{\rm cor}(p)}{\partial p}\right] = q^{\rm cor}(p)\left(+q^{\rm 2nd}_{\rm e^\pm}(p)\right)\,, \tag{4}$$

with the momentum diffusion coefficient $D(p) = p^2/\tau^{\rm cor}_{\rm acc}$. Here, the primary source rate $q^{\rm cor}(p) \propto \delta(p-p_{\rm inj})$, with an initial momentum $p_{\rm inj}$ that corresponds to a Larmor radius that matches about the smallest possible scales reached by the turbulent cascade. Note that this momentum is different for electrons and protons due to their different rest mass. In case of primary particles with $p_{\rm inj} \ll p_{\rm eq}$, where the equilibrium momentum is defined by $\tau^{\rm cor}_{\rm acc}(p_{\rm eq}) = \tau^{\rm cor}_{\rm cool}(p_{\rm eq})$, the solution of Eq. (4) yields [13]

$$n^{\rm cor}(p > p_{\rm inj} \ll p_{\rm eq}) \propto p^2\, \exp\left[-(1/a)(p/p_{\rm eq})^a\right] \tag{5}$$

with $a = 2 - \varkappa - r$, where the momentum dependence of the dominant loss process scales as $\tau^{\rm cor}_{\rm cool} \propto p^r$. In the case of CR electrons and positrons within the AGN corona, $p_{\rm eq}$ is typically quite small ($\sim 1\,{\rm MeV}/c$), so that a dominant contribution from secondary electrons and positrons with $p_{\rm inj} \gg p_{\rm eq}$ is expected. In that case, we obtain a spectral contribution at $p \gg p_{\rm eq}$ that is determined from the spectral behavior of the hadronic production rate of the secondaries as well as the dominate cooling process at these energies. Note that due to the hard CR proton spectra, the monochromatic approximation of the Bethe-Heitler process [14] as it is used in E+22, is not appropriate at low energies, so that we use the more detailed Born approximation of this process as given by Ref. [15].

To normalize the CR proton spectrum, we adopt that the CR pressure $P_{\rm cr} = \int {\rm d}p'\; n^{\rm cor}(p')\,p'\,c/3$ within the corona is a fraction $f_{\rm gas}$ of the gas pressure $P_{\rm gas} = n_{\rm gas}\,k_{\rm B}\,\theta_{\rm gas}$, i.e. $P_{\rm cr} = f_{\rm gas}\,P_{\rm gas}$. In case of the CR electron density we adopt—for the corona as well as the starburst ring—a quasi-neutral environment so that

$$\int_{T_{\rm inj}}^{\infty} {\rm d}T\; n_{\rm e}\left(p(T)\right)\,\frac{{\rm d}p}{{\rm d}T} = \int_{T_{\rm inj}}^{\infty} {\rm d}T\; n_{\rm p}\left(p(T)\right)\,\frac{{\rm d}p}{{\rm d}T}\,, \tag{6}$$

where the non-relativistic kinetic energy $T_{\rm inj}$ refers to $p_{\rm inj}$ for the corona and to the kinetic energy of the accelerating shock in case of the starburst.

In comparison, the spectral behavior of the CRs is quite different in those two environments: Within the starburst ring we expect a soft spectrum with $n^{\rm str}(p) \propto p^{-s-\delta}$, where $\delta > 0$ depends on the dominant loss process, whereas in the AGN corona we obtain $n^{\rm cor}(p_{\rm inj} < p < p_{\rm eq}) \propto p^2$, so that the spectrum is in this energy range universal and much harder.[2]

Using the previously introduced spectral energy distribution of CR protons and electrons we determine the non-thermal emission of those particles from radio to gamma-ray energies. Hereby, both emission regions are considered to be spherically symmetric and homogeneous. Thus, the resulting emission (ϵ_m) and absorption (α_m) coefficients—whose details can be found in E+22—of the messenger particle m are spatially constant, so that the spectral energy flux from a source at a distance d is given by

$$F_m(E_m) = \frac{E_m}{4\pi\, d^2}\, \epsilon_m(E_m)\, V_{\rm eff}(E_m)\,. \tag{7}$$

Here

$$V_{\rm eff}(E_m) = \int {\rm d}^3 r\; \exp\left(-\alpha_m(E_m)\, |\vec{r}_{\rm s} - \vec{r}|\right)\,, \tag{8}$$

denotes the effective emission volume, where $\vec{r}_{\rm s}$ represents an arbitrary position on the surface of the emission volume.

3. Observational Data

The previously introduced model includes the outer starburst ring (at about 1 kpc distance from the core) as well as the AGN corona in the center (with an extension of at least ~ 0.1 mpc), hence all of potential emission sites in between (such as the pc scale jet/wind emission, see e.g. [8]) cannot be taken into account. Therefore, the chosen multi-messenger dataset of NGC 1068 needs to ensure that: (i) it matches the spatial scales of the emission sites in our model, (ii) the data itself matches the same spatial scales at different wavebands, and (iii) it is related to non-thermal emission. Moreover, we account for the latest distance measurement by Ref. [16] that accurately accounts for the peculiar motion of our Galaxy away from the local void yielding a distance of NGC 1068 of $d = 10.1 \pm 1.8$ Mpc, so that $1'' \sim 50$ pc. Thus, the observational data that is used in the following consists of:

Observational data associated to the starburst ring

(i) In *the radio band*, i.e. at 2, 6 and 20 cm, VLA has observed the large scale emission at a distance between $10''$ (~ 0.5 kpc) and $25''$ (~ 1.2 kpc) with respect to the nucleus, as already used in E+22.

(ii) In *the IR band* a bolometric mid-infrared luminosity of $L_{\rm IR} = 2.4^{\pm 0.4} \times 10^{44}$ erg s^{-1} (using a source distance of 10.1 Mpc) is adopted, referring to an isotropic, diluted modified blackbody radiation field (see E+22 for more details).

(iii) In *the X-ray band* the Chandra X-ray Observatory [17] provides a measurement of the $(0.1 - 10)$ keV flux between a nuclear distances of $5''$ (~ 0.25 kpc) and $60''$ (~ 3 kpc) showing that above about 2 keV an additional power-law contribution (of potentially non-thermal origin) is needed. But since a major flux contribution emerges from small nuclear distances that cannot be associated to the starburst ring, we use these observations above 2 keV only as an upper limit.

[2]Note, that this is only the case for a very inefficient particle escape from the acceleration site—see Ref. [13] for more details.

Observational data associated to the corona None of the current observatories has a sufficient spatial resolution to resolve the corona region of NGC 1068. Therefore, all of the subsequently used data should be taken with a grain of salt.

(i) In *the radio and IR band* we use the data from a recent work by Ref. [18], where all the available Atacama Large Millimeter/ submillimeter Array (ALMA) archival data of the nuclear region of NGC 1068 has been analyzed with a beamsize of $< 0''.1$. In addition also the VLA and VLBA data from Ref. [8, 19, 20] of the nuclear region (typically referred to as S1) is summarized, which however, show a significantly different beam size—in particular the 5 GHz VLA data. There is no clear evidence of non-thermal emission at these frequencies, so that we adopt a contribution by free-free emission from dense disk winds heated by X-rays from the corona, as suggested by Ref. [8]. But it is clear that in particular in the submillimeter band not all of the spectral features can be explained by this approach, see e.g. [18].

(ii) In *the X-ray band* the high X-ray luminosity provides a clear hint of the coronal activity, since the hot thermal electrons (with temperatures of $\sim 10^9$ K) in the corona can inverse Compton scatter the UV photons from the disk to those frequencies. Due to the viewing angle, the observed flux is even already attenuated by the torus yielding an *intrinsic* luminosity at $(2-10)$ keV of [21] $L = 3.4^{+3.4}_{-2.0} \times 10^{43}$ erg/s (using a source distance of 10.1 Mpc). Its spectral behavior can be described by a power law with an exponential cutoff, that can be estimated empirically from the given Eddington ratio (bolometric to Eddington luminosity, $L_{\rm bol}/L_{\rm Edd}$) according to Ref. [22, 23]. Between 1 eV and 6 keV, we use the parametrized model from Ref. [24] to include also the UV photons from the disk. As in E+22, this UV-to-X-ray field is used as a constant photon background within our model.

Observational data of unclear origin At high γ-ray and neutrino energies the spatial origin within NGC 1068 cannot be resolved, so that it can in principle originate from both corona and starburst ring.

(i) In the *high γ-ray band* there are measurements from Fermi-LAT up to 100 GeV as well as two upper limits at $(100-300)$ GeV, and additionally some upper limits from the MAGIC telescope at higher energies, as already used in E+22.

(ii) The *high energy neutrino signal* between about $(1.5-15)$ TeV, as recently observed by the IceCube Neutrino Observatory [1], yielding a muon neutrino flux normalization at 1 TeV of $(5.0 \pm 1.5) \times 10^{-11}$ TeV^{-1} cm^{-2} s^{-1} as well as a soft spectrum ($\propto E_\nu^{-3.2\pm0.2}$) in case of a power-law.

4. Results

Guided by the best-fit results from E+22, we adjust the parameters $(s,\, f_{\rm SN},\, n_{\rm gas},\, B,\, \eta)$ of the starburst ring and $(R_{\rm cor},\, f_{\rm gas},\, n_{\rm gas},\, B,\, \eta)$ of the AGN corona to obtain a good agreement with the observational data. In case of the starburst contribution, we obtain no major changes compared to the E+22 results, as the additional upper limit in the X-ray has already been in agreement with the previous results. But in case of the necessary contribution from the AGN corona, we recognize that a significantly lower CR pressure $P_{\rm cr}$ on the order of only a few percentages or less is needed. This results from the much hard spectral behaviour of the CR protons, which we obtained from the proper treatment of the stochastic acceleration process. Moreover, this also leads to a much harder spectral behavior of the neutrino flux at $E_\nu \lesssim 1$ TeV compared to the E+22 result. The γ-ray data is still explained predominantly by the starburst ring, where a soft acceleration spectrum (with $s \simeq 2.35$) avoids the need (due to the upper limits at $\gtrsim 50$ GeV) for a high-energy cutoff. However, that leaves is a minor discrepancy at about 15 GeV. In the submillimeter range of the central nucleus, synchrotron self-absorption yields a sharp cutoff of the coronal synchrotron emission (which is dominated by secondary electrons and positrons), so that only at 691 GHz a significant amount of this emission is left. At lower frequencies the free-free emission of the extended diffuse ionized gas is needed to explain the data, so that especially the spectral details of the VLBA data of the S1 region are not accurately reproduced.

But overall, the multi messenger data is—without a detailed fitting approach—already explained quite well by our updated model showing that the starburst ring and the AGN corona is needed to understand the high energy phenomena of NGC 1068.

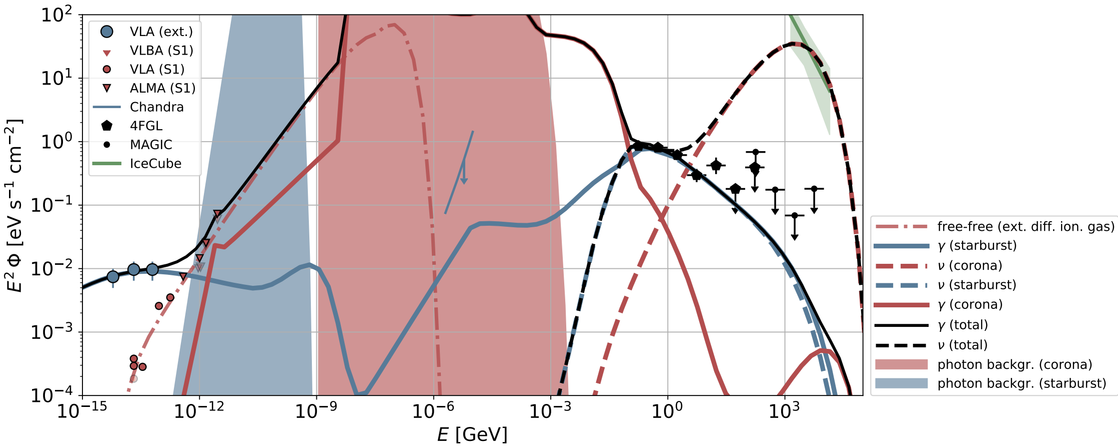

Figure 1: The model predictions of the *photon and neutrino* SED of NGC 1068 with respect to the multi-messenger data as given in Sect. 3. Note that the torus attenuation—which becomes relevant at energies $\lesssim$ 1 MeV—is not taken into account here.

5. Conclusions and Discussion

In this work, we updated the spatially homogeneous, spherically symmetric, steady state two-zone model for AGN-starburst composite galaxies, that has first been introduced by E+22. We now properly account for the stochastic acceleration process within the AGN corona (in case of an inefficient particle escape) as well as the Bethe-Heitler pair production. Moreover, we used some updates of the multi-messenger data of NGC 1068, such as the recently detected neutrino flux, and present a manual fit to these data. Similar to the E+22 results, the γ-ray emission above a few $\times$100 MeV results predominantly from the starburst region, whereas the high-energy neutrinos at TeV energies must originate from the coronal region. But in contrast to previous results a significantly lower CR pressure within the corona is needed and a strong decline of the neutrino flux *towards lower energies* at about 1 TeV is obtained. In the centimeter to submillimeter band we still account for an additional contribution by an extended diffuse ionized gas with a spatial extension of $\sim$ 1 pc that, however, is of unclear origin (see Ref. [18] for a more detailed discussion). To what extent this contribution is actually needed or if it can be replaced completely by a contribution from the base of the jet or the torus, needs to be clarified in future investigations with a more detailed fitting approach.

Acknowledgements

BE, SS, RJD, and JT acknowledge support from the Deutsche Forschungsgemeinschaft (DFG): this work was performed in the context of the DFG-funded Collaborative Research Center SFB1491 "Cosmic Interacting Matters - From Source to Signal", project no. 445052434.

References

[1] IceCube Collaboration *Science* **378** (2022) 538.

[2] K. Murase and E. Waxman *Phys. Rev. D* **94** (2016) 103006.

[3] B. Eichmann and J. Becker Tjus *Astrophys. J.* **821** (2016) 87.

[4] Y. Inoue, D. Khangulyan and A. Doi *Astrophys. J. Lett.* **891** (2020) L33.

[5] K. Murase, S.S. Kimura and P. Mészáros *Phys. Rev. Lett.* **125** (2020) 011101.

[6] A. Kheirandish, K. Murase and S.S. Kimura *Astrophys. J.* **922** (2021) 45.

[7] B. Eichmann, F. Oikonomou, S. Salvatore, R.-J. Dettmar and J.B. Tjus *Astrophys. J.* **939** (2022) 43.

[8] J.F. Gallimore, S.A. Baum and C.P. O'Dea *Astrophys. J.* **613** (2004) 794.

[9] J.F. Gallimore, D.J. Axon, C.P. O'Dea, S.A. Baum and A. Pedlar *Astron. J.* **132** (2006) 546.

[10] J.P. Lenain, C. Ricci, M. Türler, D. Dorner and R. Walter *Astron. Astrophys.* **524** (2010) A72.

[11] S. Inoue, M. Cerruti, K. Murase and R.-Y. Liu *arXiv e-prints* (2022) arXiv:2207.02097.

[12] G.E. Romero, A.L. Müller and M. Roth *Astron. Astrophys.* **616** (2018) A57.

[13] Ł. Stawarz and V. Petrosian *Astrophys. J.* **681** (2008) 1725.

[14] Y. Zheng, C. Yang and S. Kang *Astronomy & Astrophysics* **585** (2016) A8.

[15] G.R. Blumenthal *Phys. Rev. D* **1** (1970) 1596.

[16] R.B. Tully, E.J. Shaya, I.D. Karachentsev et al. *Astrophys. J.* **676** (2008) 184.

[17] A.J. Young, A.S. Wilson and P.L. Shopbell *Astrophys. J.* **556** (2001) 6.

[18] T. Michiyama, Y. Inoue and A. Doi *arXiv e-prints* (2023) arXiv:2306.15950.

[19] J.F. Gallimore, S.A. Baum, C.P. O'Dea and A. Pedlar *Astrophys. J.* **458** (1996) 136.

[20] W.D. Cotton, W. Jaffe, G. Perrin and J. Woillez *Astron. Astrophys.* **477** (2008) 517.

[21] A. Marinucci, S. Bianchi, G. Matt et al. *Mon. Not. Roy. Astron. Soc.* **456** (2016) L94.

[22] C. Ricci, L.C. Ho, A.C. Fabian et al. *Mon. Not. Roy. Astron. Soc.* **480** (2018) 1819.

[23] B. Trakhtenbrot, C. Ricci, M.J. Koss et al. *Mon. Not. Roy. Astron. Soc.* **470** (2017) 800.

[24] L.C. Ho *Annu. Rev. Astron. Astrophys.* **46** (2008) 475.